

Design of an Integrated Optical Switch Based on Liquid Crystal Infiltration

Francesco Riboli, Nicola Daldosso, Georg Pucker, Alberto Lui, and Lorenzo Pavesi

Abstract—We present the design and simulation of a novel Fabry–Pérot optical switch based on liquid crystal infiltration integrated in a high index-contrast silicon-on-insulator waveguide. Careful optimization of the cavity geometry allows designing a device with a resonance peak transmission of 95% and a resonance peak linewidth of 1.7 nm. This kind of device is designed to be fully CMOS compatible and can be used as a building block of a more complex integrated optical circuit.

Index Terms—CMOS integrated circuits, Fabry–Pérot resonators, liquid crystals (LCs), optical switches, waveguides.

I. INTRODUCTION

VARIOUS silicon compatible photonic devices have been studied in these last years [1]. Among these, one that deserves a particular attention is a device that is able to route the optical signal among different optical channels, i.e., an optical router. The best option for a router is a reconfigurable optical router for which the routing is dynamically addressed. The key component of an optical router is the optical switch, which transmits or blocks the optical signal depending on the routing protocol. Optical switches can be done either by using moving mirrors or by exploiting the wavelength dependence of optical filters. Also for the optical switch, the aim is reconfigurable switching.

In this work we present simulation results on the design of an optical switch realized with silicon-on-insulator (SOI) waveguides. The technical feasibility of the device is not addressed here. However we designed it keeping in mind the limit of CMOS processing of silicon. Indeed the fabrication of this kind of device is underway in our laboratories. The optical switch is based on a Fabry–Pérot (FP) resonator composed of two symmetric distributed bragg reflectors (DBR) and a cavity. The cavity is filled with a material whose refractive index can be changed by applying an electric field; hence, the cavity resonance is tunable. Thanks to their electrooptic properties, we propose to use liquid crystals (LC) to fill the cavity. The basic operation of this device (tunable FP) has been previously demonstrated in a system realized by two DBR mirrors bonded together [2]. Resonance shift of the order of 100 nm by increasing the bias from 4 to 10 V was observed when E7 LCs are used to fill the spacing between the mirrors. Similar devices

have been proposed and realized by other groups, too [3]–[5]. Here we aim to present the design of an integrated optical switch and its optimization to obtain minimum insertion losses and bandwidth. All the results reported are simulation results.

II. DESIGN OF THE DEVICE AND DEFINITION OF THE PARAMETERS

Fig. 1(a) shows a schematic of the ideal device: two SOI waveguides are coupled through a FP cavity formed with two DBR separated by a layer filled with LCs. The waveguides are formed by a 5- μm -thick Si core. The FP cavity is formed by two three-periods DBR (based on Si–SiO₂ $\lambda/4$ -thick stacks) separated by a λ -thick cavity. The cavity is filled with LCs which are simulated by introducing a medium with a given refractive index n_{LC} . In our simulation, we assume that the optical axis of LC is perpendicular to the propagation direction of light and that the LC are oriented so that TE mode in the cavity is parallel to the extraordinary ray. In addition, we assume, that the refractive index is constant for the whole spacer distance. The electrooptic behavior of the LC is simply simulated by changing the refractive index value.

Fig. 1(b) shows the transmission spectra for a few values of n_{LC} ¹ of the ideal device when the fundamental TE₀ mode of the input waveguide is excited. For $n_{\text{LC}} = 1.65$, a peak transmission of 76% (1.2-dB insertion losses) and a full-width at half-maximum (FWHM) of 1.9 nm are observed. Varying the refractive index of the LC to reproduce the effect of an external electric field, we observe a wavelength shift of the peak. This is the basic principle of the reconfigurable optical switch: the resonance of the FP will determine which optical signal is transmitted (switch closed) or blocked (switch open). Let us further note in Fig. 1(b) that the TE₀ peak transmission increases when n_{LC} increases. Indeed the cavity layer behaves as a waveguide because n_{LC} is larger than the refractive index of the SiO₂ cladding layer. Increasing n_{LC} , the cavity mode becomes more confined and, consequently, the insertion losses decrease.

Even in the perfectly symmetric structure, where air is used as bottom and top cladding layer, the transmission of the TE₀ mode is at maximum 92%. Fig. 1(c) shows the plot of the TE field (backward and forward) in the device. This plot allows to look at the causes of the insertion losses: light channelled in the waveguide is partially transmitted through the cavity in the output waveguide, but it is also partially reflected back by the DBR, and partially is radiated in the air and cladding layers

¹This value has been chosen because of the large availability of LCs with refractive index between 1.6 and 1.7. For example, E7 has $n_e = 1.75$ and $n_o = 1.523$.

Manuscript received January 28, 2005; revised May 17, 2005. This work was supported by PAT through the PROFILL project.

F. Riboli, N. Daldosso, and L. Pavesi are with the Department of Physics, University of Trento, Trento 38050, Italy (e-mail: riboli@science.unitn.it; daldosso@science.unitn.it; pavesi@science.unitn.it).

G. Pucker and A. Lui are with Microsystems Division, ITC-IRST, Trento 38050, Italy (e-mail: pucker@itc.it; lui@itc.it).

Digital Object Identifier 10.1109/JQE.2005.853363

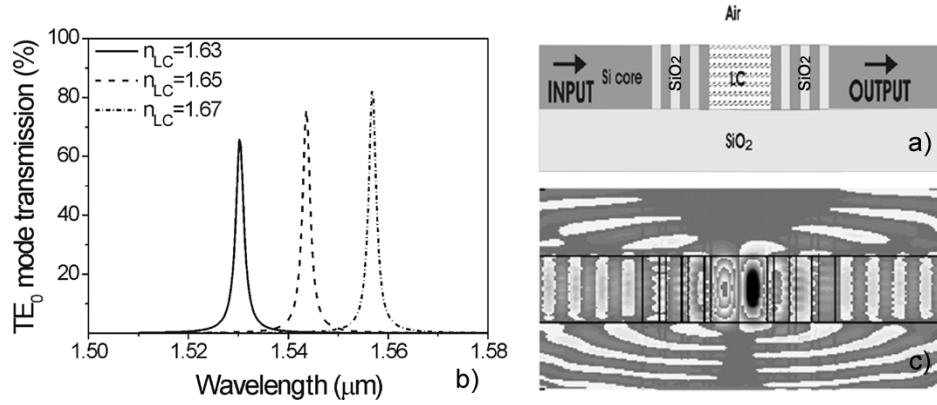


Fig. 1. (a) Scheme of the cross section of the ideal device. LC refers to the cavity layer filled with LCs. The cavity length is λ where the refractive index of the LCs is 1.65. (b) Transmission spectra of the fundamental TE_0 mode for three different values of refractive index of liquid crystal n_{LC} . (c) Total (backward and forward) TE field profile having enhanced the losses.

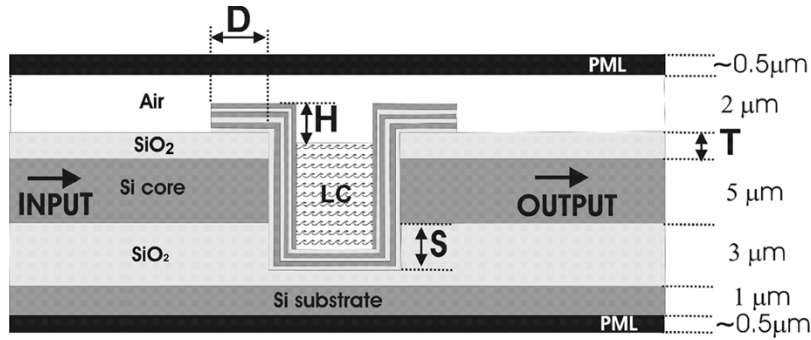


Fig. 2. Cross-section of the proposed device. The various parameters, optimized in the simulations, are D , H , T , S and are defined in the text.

due to the different mode profiles for the fundamental mode propagating through the FP structure.

These first results obtained with an ideal structure show that the optimization of the device has to concentrate on those parameters which allow to match the mode profile all along the structure and, thus, to reduce the radiation losses.

We aim to design an optical switch that could be fabricated using standard CMOS technology and SOI wafers. In order to preserve CMOS compatibility, the design of the device assumes that the LCs in-fill into the cavity is a back-end process. Indeed all the steps to realize the device with an empty cavity are well within the possibilities of nowadays CMOS processing [1]. The cross section of the actual device will be closer to the one in Fig. 2 than the one in Fig. 1. A silicon waveguide, $5 \mu\text{m}$ thick, is formed by using two SiO_2 cladding layers: the bottom cladding layer thickness is fixed at $3 \mu\text{m}$ to guarantee isolation from the Si substrate while the thickness of the top cladding is an optimization parameter named T . In the simulation we have also considered the presence of the substrate by adding a $1 \mu\text{m}$ thick Si layer on the bottom. On the top of the structure, there are $2 \mu\text{m}$ of air and $0.5\text{-}\mu\text{m}$ of a perfect matching layer (PML) layer [6] to prevent spurious reflection at boundaries. The DBR mirrors are composed by three periods of alternating $\lambda/4$ SiO_2 -Si layers. Si and SiO_2 thicknesses of 110 and 270 nm, respectively, are used for a target wavelength of $\lambda = 1550$ nm. Note that to realize the electrodes to polarize the LCs in the cavity layer, the last Si layer of the DBR is not continuous. The DBR are deposited by using conformal growth on a trench opened in the SOI wave-

guide. The cavity layer is filled with LCs, and has a physical thickness of 940 nm when the optical thickness is λ with a refractive index of LCs of 1.65 .

In the fabrication process we can control various parameters that we use in the simulation as optimization parameters as follows (Fig. 2):

- T thickness of the top cladding;
- S depth of the cavity in the bottom cladding layer;
- D length of the overlap of the Si- SiO_2 multilayers on the top cladding due to the conformal growth;
- H height of the empty layer in the cavity.

In particular, S and T determine both the position and spatial extension of the DBR and, consequently, determine the spatial profile of the Bloch modes, which are the optical modes propagating through the DBRs. D regulates the resonance properties of the extra cavity (named top FP or cavity 2) which forms on the top cladding. H determines the optical confinement factor and the modal profile of the guided modes in the cavity layer.

III. SIMULATION METHOD

We perform a two-dimensional characterization of the ridge waveguide by using the effective-index method. This choice reduces the computation difficulties and increases the accuracy of the simulation results. The target of the optimization is to maximize the resonant peak transmission intensity of the fundamental waveguide TE_0 mode from the input to the output waveguide, i.e., to reduce the insertion losses of the switch.

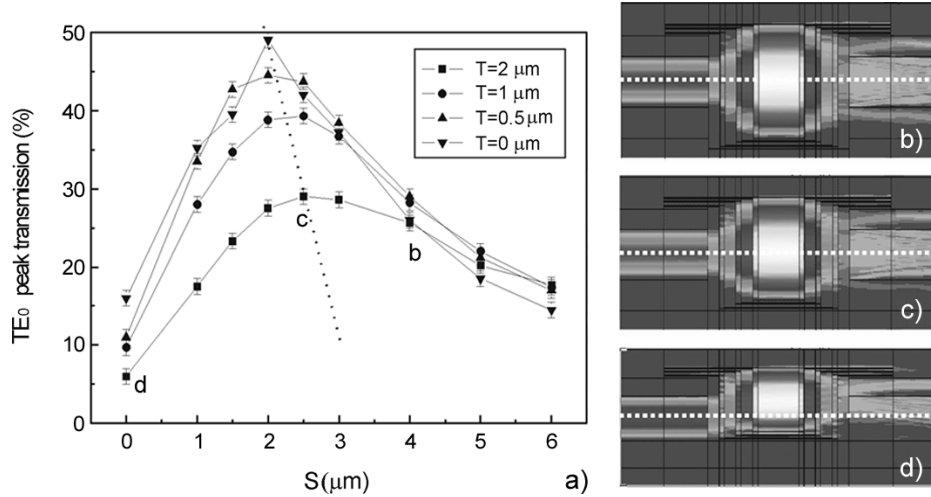


Fig. 3. (a) TE₀ peak transmission as a function of S for various T values. The dotted line is a guide for the eye showing the shift of the curve maximum decreasing the thickness of the top cladding (T). Intensity profile of the forward TE power (b) for $S = 4 \mu\text{m}$ and $T = 2 \mu\text{m}$; (c) for $S = 3 \mu\text{m}$ and $T = 2 \mu\text{m}$; (d) for $S = 0 \mu\text{m}$ and $T = 2 \mu\text{m}$. The white dotted horizontal line indicates the center of the waveguide.

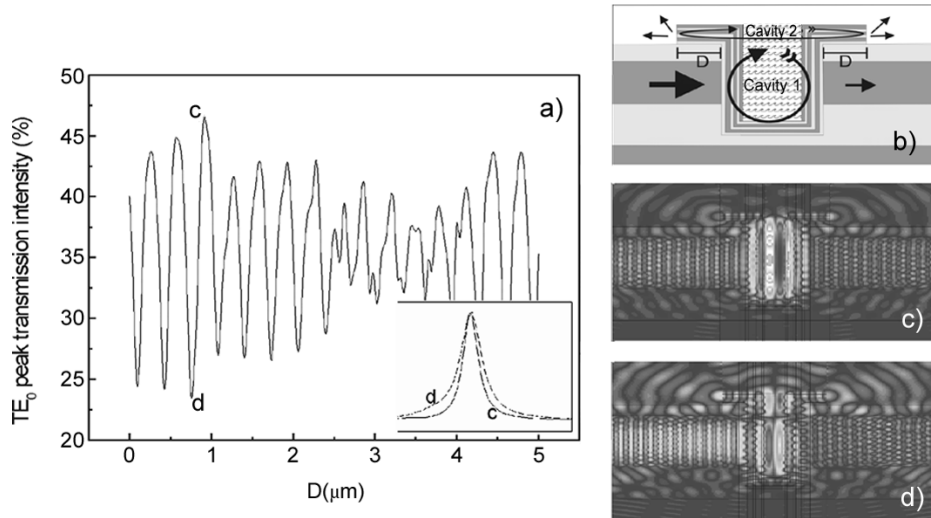


Fig. 4. (a) TE₀ peak transmission intensity as a function of D for $S = 2 \mu\text{m}$, $T = 1 \mu\text{m}$, and $H = 0 \mu\text{m}$. (b) Cross section of the device with indicated the main cavity (cavity 1) and the top FP resonator (cavity 2). TE field profile at the resonance wavelength for the case of (c) detuned and (d) tuned cavity 2. The inset in (a) shows the normalized transmission spectra of the TE₀ mode for the detuned (continuous line) and tuned situation (dotted line).

The architecture of the device is particularly suitable to be simulated with the eigenmode expansion (EME) method [7], [8], also known as Fourier modal analysis. In fact, the EME method is particularly suited for those structures that can be viewed as a series of slices with invariant refractive index profile along the direction of propagation of light. This is just the case of the device shown in Fig. 2. The EME method is a bidirectional propagation method that solves exactly the Maxwell equations. Its accuracy depends on the number of enabled eigenmodes in each slice. We have used a commercial software to perform the simulations.²

In the simulation, the device is represented by 17 different slices, of which only nine are independent; about 120 eigenmodes are enabled in each slice. With this number of modes we estimate an error of 0.5%–1% on the transmission values due to the finite basis set. The input planar waveguide supports about

30 guided modes. In the simulation, we excite only the fundamental TE₀ mode of the input waveguide and we perform a wavelength scan around the resonance wavelength and record the TE₀ mode intensity in the output waveguide. All the radiating modes are absorbed by the PML layer without influencing the spectrum of the TE₀ mode.

IV. RESULTS OF THE FIRST OPTIMIZATION RUN

We fix $n_{LC} = 1.65$, $D = 23 \mu\text{m}$, $H = 0 \mu\text{m}$, and vary S and T : S between 0 and 4 μm and T between 0 and 2 μm. The TE₀ peak transmission intensity has an inverted bell-shape as a function of S [Fig. 3(a)]. Larger values are observed for smaller T . This profile is due to the variations of the modal overlap among the cavity mode and the waveguide modes.

When both S and T are large, the cavity mode is wide and couples with several lossy channels [Fig. 3(b)]: light is radiated out of the cavity via the cladding layers and the top FP layers.

²Photon Design Software: FimmWave and FimmProp.

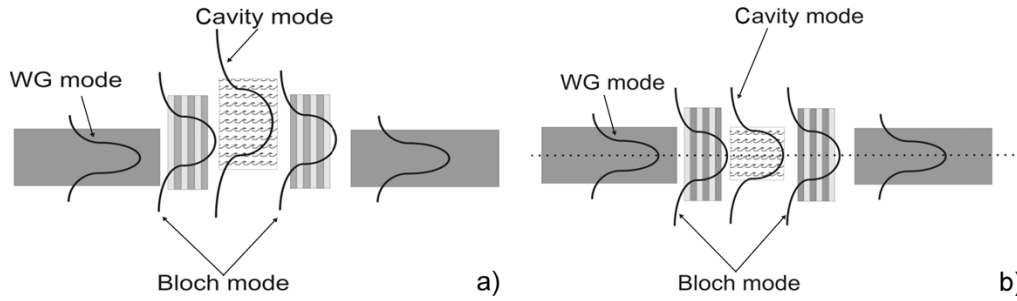


Fig. 5. Sketch of the various optical modes in our device. (a) Mismatched case. (b) Matched case.

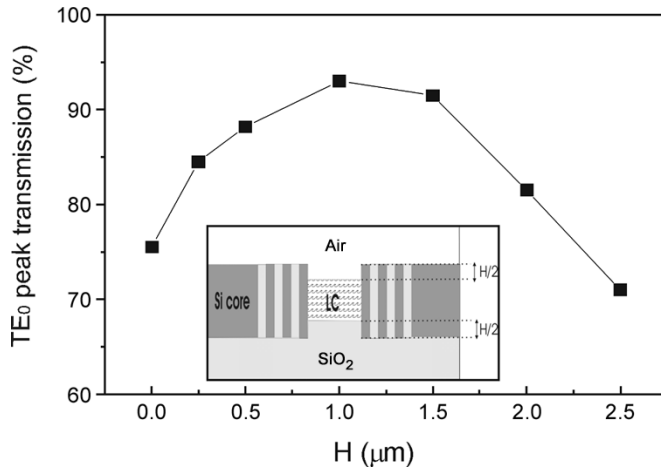


Fig. 6. TE_0 peak transmission versus H for the ideal optical switch.

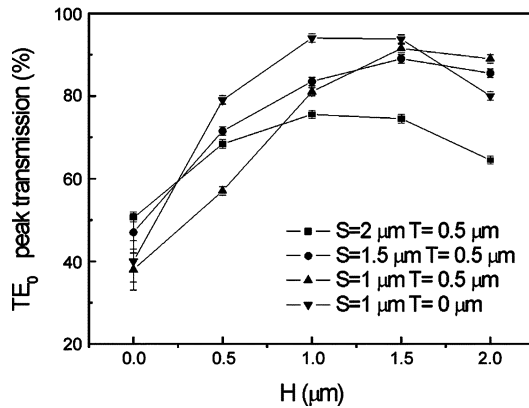


Fig. 7. TE_0 resonance peak transmission value versus H for various S and T values. D was optimized for each H , S , and T set.

This radiated light does not couple back into the output waveguide. If S is decreased, i.e., the depth of the cavity is reduced, the loss toward the bottom cladding layer is reduced due to the upward shift of the cavity mode [Fig. 3(c)].

A maximum transmission is reached for an S value where the modal overlap between the waveguide mode and the cavity mode is maximized and the coupling with the lossy channels is reduced. When the S value is further decreased, the cavity mode is further pushed upwards [Fig. 3(d)]. This causes, on one side, the decrease of the overlap among the waveguide and the cavity modes and, on the other side, the increase of the optical power radiated through the top cladding. Consequently the transmission intensity decreases significantly reaching very low values for low S values.

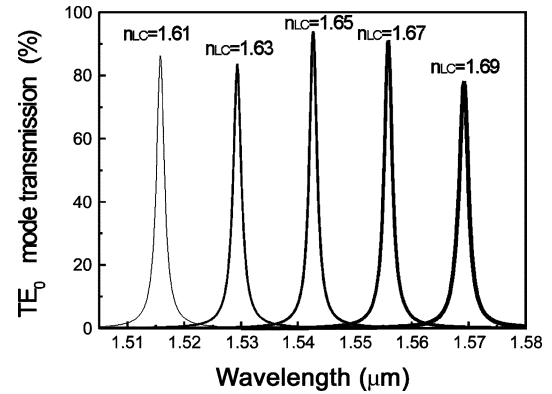


Fig. 8. TE_0 transmission spectrum for various values of the refractive index of the LCs, n_{LC} . Such n_{LC} variation correspond to a bias of few volts when the E7 LCs are used [2]. The device has $S = 1 \mu\text{m}$, $T = 0 \mu\text{m}$, $D = 23.2 \mu\text{m}$, and $H = 1.5 \mu\text{m}$. These values were chosen because during previous optimization runs, they minimized the insertion losses of the device with $n_{LC} = 1.65$.

Decreasing T , the modal overlap among the cavity mode and the waveguide modes increases, and the coupling with the lossy channels decreases. This, in turn, means an increased transmission intensity. Finally, as T is decreased, the S value of maximum transmission intensity decreases because the best symmetric overlap among the waveguide modes and the cavity mode is achieved at smaller S values.

For a fixed n_{LC} , the spectral shape of the transmission resonance depends weakly on the S and T values: the resonance is about 2.2-nm-wide and is centred at 1546 nm with an overall maximum shift of 0.2 nm for the FWHM and 2 nm for the peak position. Reducing S , a second weak resonance appears at $1535 \pm 2 \text{ nm}$ with an intensity of 1%–3.5%.

V. ROLE OF THE MULTILAYER OVERLAPPING THE TOP CLADDING

The DBR are deposited in the trench opened between the SOI waveguide by using a conformal growth (Fig. 2). Unless one uses chemical-mechanical polishing or specific masks, it is unavoidable that the deposited multilayers overlap the top cladding. Thus, we investigate the influence of these surface layers as a function of their length (D parameter).

These multilayers act as a further FP cavity due to light reflection at their edges (we refer to it as cavity 2 in Fig. 4). The top FP or cavity 2 is coupled to the main cavity via light which is channeled through the DBR layers or is diffracted at the exit of the input waveguide; thus the top FP and the main cavity form a system of side coupled resonators [Fig. 4(b)].

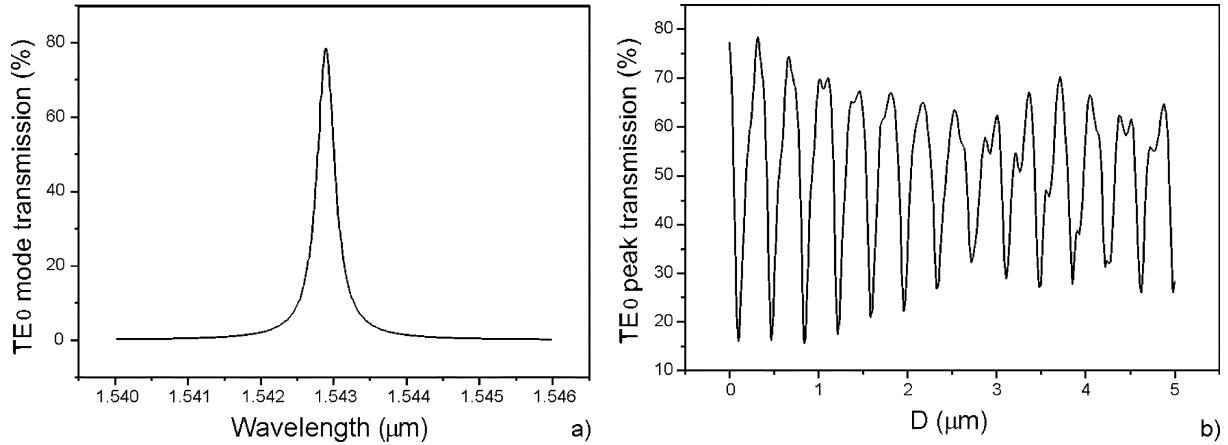


Fig. 9. (a) TE_0 transmission spectrum for an optimized device with four periods DBR. (b) TE_0 peak transmission as a function of D .

The main effect of this coupling is shown in Fig. 4(a), where the TE_0 peak transmission of the main cavity is reported as a function of D , the top FP half-length. A complicated pattern of oscillations is observed due to the complex nature of the top FP that is a system of three coupled waveguides: one for each DBR period, where the Si layer acts as core layer and the SiO_2 layers as cladding layers. These waveguides have different lengths and different couplings to the cavity mode. Fig. 4(c) and (d) are representative examples of two opposite situations: when the frequency resonances of the top FP and the main cavity are the same [Fig. 4(d)] and when they are different [Fig. 4(c)]. When the two cavities have the same resonance frequency [Fig. 4(d)], the light is stored in the top as well as in the main cavity thus resulting in an enhancement of the field intensity in the region of the top cavity. As a consequence, the transmitted intensity of the output waveguide decreases. When the frequency resonance is different, a smaller amount of light is coupled to the top cavity [Fig. 4(c)]. In this case, the light cannot escape through the top cavity and, thus, it is transmitted into the output waveguide. As a consequence the FWHM of the resonance in the detuned situation (c point) is smaller than the one in the tuned situation (d point), as shown in the inset of Fig. 4(a).

Assuming perfect and mirror-like facets for the top FP, the modulation in the transmitted intensity is as large as 20%. The coupling between the cavity and the top FP does not significantly depend on H , because the coupling occurs via the DBR.

VI. FINAL OPTIMIZATION OF THE DEVICE: MATCHING THE CAVITY MODE WITH THE BLOCH MODE

Fig. 5(a) and (b) show an hand-drawn sketch of the various mode profiles in the five sections of the device. During the optimization of the device design, we try to engineer the various mode profiles such that their overlaps at each section interface are maximized. In particular, Fig. 5(a) shows a mismatched situation that can be compared with Fig. 3(d). The profiles of the input waveguide, Bloch mode and cavity mode are totally misaligned resulting in a low transmission intensity. On the other hand, Fig. 5(b) shows the case where the profile of each mode is aligned. By changing S and T , we maximize the spatial overlap of the optical modes of the cavity, of the waveguides and, at the same time, of the Bloch modes. A fine tuning is now

needed to optimize independently the modal overlap among the Bloch modes and the cavity mode [9], [10]. This is achieved by changes in H (Fig. 2). Indeed as H is increased the height of the LCs in the cavity decreases and, hence, the cavity mode gets more confined.

We first make a simulation for the ideal case [Fig. 1(a)]. Fig. 6 reports the results for the TE_0 transmission as a function of H . Decreasing the height of the cavity layer, the modal overlap between the propagating Bloch modes and the resonant cavity mode is increased; a maximum of 93% can be achieved. A further decrease yields a transmission decrease because the optical mode extent in the cavity becomes too small to allow significant coupling of optical power through the cavity into the output waveguide.

Fig. 7 reports the results for the actual device, where the TE_0 transmission as a function of H is shown with the best values for S and T . A maximum value of 94% for the TE_0 transmission is achieved for $H = 1 \mu\text{m}$, $S = 1 \mu\text{m}$, and $T = 0 \mu\text{m}$.

VII. TRANSMISSION SPECTRUM

The device has to operate as a tuneable switch. This means that changing the refractive index of the LC by an external bias tunes the resonance wavelength. This will affect all the modal overlaps and the cavity-top FP coupling, and will increase the insertion losses. In Fig. 8, the transmission spectra of the optimized device for various values of the refractive index of the LC are shown. A resonant peak shift of 55 nm is observed when the refractive index of the LCs is varied from 1.61 to 1.69. This range of variation is practically achievable [2]. Despite some variations in the maximum transmission can be observed, its value is never lower than 78% (maximum insertion losses of 1.1 dB) with a spectral width of 1.7 nm.

To narrow further the resonance transmission peak, one can increase the number of DBR periods. This will require a fine tuning of all the parameters. The transmission spectrum of an optimized device with 4 periods in the DBR is shown in Fig. 9. Insertion losses of 0.96 dB at the resonance with a FWHM = 0.3 nm are observed. With this configuration, however the coupling strength between the top FP and the cavity increases enormously and the variation in the transmission for small variation of D becomes very large [Fig. 9(b)].

VIII. CONCLUSION

We have presented a new architecture of an integrated optical switch based on a FP cavity filled with LCs. By maximizing the overlap among the optical modes in the input-output waveguides, the Bloch modes and the cavity mode we have found very promising performances of the switch. The optimized device has a TE_0 resonant peak transmission value of about 95% with a quality factor of $\lambda/\Delta\lambda = 900$. An improved device structure with higher reflectivity mirrors shows improved quality factors up to 5160 with a slightly lower transmission of 80%. We are currently working to realize the proposed optical switch within a silicon foundry by using CMOS processing so that the simulation results reported here will be tested.

REFERENCES

- [1] L. Pavesi and D. Lockwood, *Silicon Photonics*. Heidelberg, Germany: Springer-Verlag, 2004, vol. 94, Topics in Applied Physics.
- [2] G. Pucker, A. Mezzetti, M. Crivellari, P. Bellutti, A. Lui, N. Daldosso, and L. Pavesi, "Silicon based near infrared tunable filter filled with positive or negative dielectric anisotropic liquid crystals," *J. Appl. Phys.*, vol. 96, pp. 767–769, 2004.
- [3] L. Sirlito, G. Coppola, G. Breglio, G. Abbate, G. C. Righini, and J. M. Oton, "Electro-optical switch and continuously tunable filter based on a Bragg grating in a planar waveguide with a liquid crystal overlayer," *Opt. Eng.*, vol. 41, pp. 2890–2898, 2002.
- [4] I. Del Villar, I. R. Matias, F. J. Arregui, and R. O. Claus, "Analysis of one-dimensional photonic bandgap structure with a liquid crystal defect toward development of fiber-optics tunable wavelength filters," *Opt. Exp.*, vol. 11, pp. 430–436, 2003.
- [5] A. D'Orazio, "Infiltrated photonic crystal photonic bandgap devices for switching and tunable filtering," *Fiber Integr. Opt.*, vol. 22, pp. 161–172, 2003.
- [6] J. P. Béranger, "A perfectly matched layer for the absorption of electromagnetic waves," *J. Comput. Phys.*, vol. 114, pp. 185–200, 1994.
- [7] A. S. Sudbo, "Film mode matching: a versatile numerical method for vector mode field calculation in dielectric waveguides," *Pure Appl. Opt.*, vol. 2, pp. 211–233, 1993.
- [8] —, "Film mode matching: a versatile numerical method for vector mode field calculation in dielectric waveguides," *Pure Appl. Opt.*, vol. 2, pp. 211–233, 1993.
- [9] M. Palamaru and P. Lalanne, "Photonic crystal waveguides: Out-of-plane losses and adiabatic modal conversion," *Appl. Phys. Lett.*, vol. 78, pp. 1466–1469, 2001.
- [10] J. Ctyroky, "Photonic bandgap structures in planar waveguides," *J. Opt. Soc. Amer. A*, vol. 18, pp. 435–441, 2001.



Francesco Riboli was born in Firenze, Italy, on May 30, 1976. He received the Laurea degree in physics at the University of Florence, Florence, Italy, in March 2001. In November 2002, he began working toward the Ph.D. degree in the Physics Department, University of Trento, Trento, Italy, under the supervision of L. Pavesi.

After receiving the Laurea degree, he worked for one year at the University of Florence, Florence, Italy. His main research interests include Si-based photonic components for integrated optics (photonic crystals, optical switches, and waveguides) and cold atoms physics (both theoretical and experimental).



Nicola Daldosso was born in Verona, Italy, on April 6, 1972. He received the Laurea degree in physics from the University of Trento, Trento, Italy, in March 1997, and the Ph.D. degree in physics of matter from the Université J. Fourier, Grenoble, France, in 2001.

From 1998 to 2000, he was at the Italian Beamline GILDA at European Synchrotron Radiation Facilities (ESRF), Grenoble, France. Since 2001, he has been with the Physics Department, University of Trento. His research interests include structural and optical properties of nanostructures materials, in particular silicon nanocrystals, and, more recently, integrated optoelectronics on silicon.



Georg Pucker was born in Graz, Austria, in 1967. He received the Ph.D. degree in technical chemistry from the Graz Technical University, Graz, Austria, in 1996.

From October 1996 to January 2001, he worked first as a Postdoctoral student, then as Researcher at the Physics Department, University of Trento, Italy. Since January 2001, he has been a researcher in the Microsystem Division, IRST-ITC, Trento, Italy. His current research includes integrated silicon photonics, planar waveguides, Fabry–Pérot cavities, and properties of silicon-rich-oxide and related materials.



Alberto Lui received the Laurea degree from University of Bologna, Bologna, Italy, in 1987.

In 1989, he joined the Microsystems Division, ITC-IRST, Trento, Italy, where he has been involved in the development of various technologies (CCD, C-MOS, ISFET, MEMS). He's responsible of the Characterization Laboratory and of the Silicon Photonics activities. His research interest include silicon photonics devices development, processes, and devices reverse engineering and failure analysis.



Lorenzo Pavesi received the M.S. degree from the University of Trento, Trento, Italy, in 1985 and the Ph.D. degree from the Ecole Polytechnique Federale de Lausanne, Lausanne, Switzerland, in 1990, both in physics.

He became Assistant Professor in 1990, an Associate Professor in 1999, and Full Professor of experimental physics in 2002 at the University of Trento. He teaches several classes both at the Science as well as at the Engineering Faculties of the University of Trento. He founded the research activity in semiconductor optoelectronics at the University of Trento and started several laboratories of optical spectroscopy, growth, and advanced treatment of materials. His main research interests include the optical properties of semiconductors, the properties of III–V semiconductors grown on high index surfaces, the role of hydrogen in semiconductors, the diffusion of impurities in GaAs, the disorder in superlattices, and the photonic crystals. During the last few years, he concentrated on Si-based optoelectronics and photonics. He is an author or coauthor of more than 200 papers, author of several reviews, editor of seven books, author of one book, and holds three patents.